MIT Libraries | DSpace@MIT

MIT Open Access Articles

High-speed ultra-broad tuning MEMS-VCSELs for imaging and spectroscopy

The MIT Faculty has made this article openly available. ***Please share*** how this access benefits you. Your story matters.

Citation: Jayaraman, V., B. Potsaid, J. Jiang, G. D. Cole, M. E. Robertson, C. B. Burgner, D. D. John, et al. "High-Speed Ultra-Broad Tuning MEMS-VCSELs for Imaging and Spectroscopy." Edited by Ulrich Schmid, José Luis Sánchez de Rojas Aldavero, and Monika Leester-Schaedel. Smart Sensors, Actuators, and MEMS VI (May 17, 2013). © 2013 SPIE

As Published: http://dx.doi.org/10.1117/12.2018345

Publisher: SPIE

Persistent URL: http://hdl.handle.net/1721.1/86409

Version: Final published version: final published article, as it appeared in a journal, conference proceedings, or other formally published context

Terms of Use: Article is made available in accordance with the publisher's policy and may be subject to US copyright law. Please refer to the publisher's site for terms of use.

Massachusetts Institute of Technology

Invited Paper

High-speed ultra-broad tuning MEMS-VCSELs for imaging and spectroscopy

V. Jayaraman[a*], B. Potsaid[b], J. Jiang[b], G. D. Cole[c], M. E. Robertson[a], C. B. Burgner[a], D. D. John[a], I. Grulkowski[d], W. Choi[d], T.H. Tsai[d], J. Liu[d], B.A. Stein[e], S.T. Sanders[e], J.G. Fujimoto[d], and A.E. Cable[b]. a. Praevium Research, Inc. 5266 Hollister Avenue Suite 224, Santa Barbara, CA 93111, USA. b. Thorlabs, 56 Sparta Avenue Newton, NJ 07860, USA. c. Advanced Optical Microsystems, 1243 West El Camino Real, Mountain View, CA 94040, USA. d. Department of Electrical and Computer Engineering, Massachusetts Institute of Technology, 77 Massachusetts Avenue, Cambridge, MA 02139, USA. e. University of Wisconsin-Madison, 1500 WI 53715, USA.

ABSTRACT

In the last 2 years, the field of micro-electro-mechanical systems tunable vertical cavity surface-emitting lasers (MEMS-VCSELs) has seen dramatic improvements in laser tuning range and tuning speed, along with expansion into unexplored wavelength bands, enabling new applications. This paper describes the design and performance of high-speed ultra-broad tuning range 1050nm and 1310nm MEMS-VCSELs for medical imaging and spectroscopy. Key results include achievement of the first MEMS-VCSELs at 1050nm and 1310nm, with 100nm tuning demonstrated at 1050nm and 150nm tuning at shown at 1310nm. The latter result represents the widest tuning range of any MEMS-VCSEL at any wavelength. Wide tuning range has been achieved in conjunction with high-speed wavelength scanning at rates beyond 1 MHz. These advances, coupled with recent demonstrations of very long MEMS-VCSEL dynamic coherence length, have enabled advancements in both swept source optical coherence tomography (SS-OCT) and gas spectroscopy. VCSEL-based SS-OCT at 1050nm has enabled human eye imaging from the anterior eye through retinal and choroid layers using a single instrument for the first time. VCSEL-based SS-OCT at 1310nm has enabled real-time 3-D SS-OCT imaging of large tissue volumes in endoscopic settings. The long coherence length of the VCSEL has also enabled, for the first time, meter-scale SS-OCT applicable to industrial metrology. With respect to gas spectroscopy, narrow dynamic line-width has allowed accurate high-speed measurement of multiple water vapor and HF absorption lines in the 1310nm wavelength range, useful in gas thermometry of dynamic combustion engines.

Keywords: Optical coherence tomography, MEMS-VCSELs, Gas spectroscopy, Tunable lasers, Engine thermometry

I. INTRODUCTION

Rapidly swept, widely tunable lasers at a variety of wavelengths have long been recognized as a critical enabling technology in optical imaging and optical spectroscopy[1, 2]. Two key example applications are swept source optical coherence tomography (SS-OCT)[3], and transient gas spectroscopy for thermometry of combustion engines[4]. Desirable tunable laser parameters include wide tuning range, high and variable sweep speed, narrow dynamic line-width, high output power, and wavelength flexibility[1, 2]. The benefits of these features are as follows. In SS-OCT, high sweep rate enables real-time acquisition of large volumetric data sets, reduces sensitivity to patient motion, and allows imaging of dynamically varying physiological processes. High output power enhances signal-to-noise and image quality, with 30-60mW desirable for many 1310nm vascular and cancer imaging applications, and 15-25mW desirable for many 1050nm ophthalmic SS-OCT applications. Variable sweep rates are desirable in SS-OCT, since limited detection bandwidth forces a tradeoff between imaging range and wavelength sweep rate[5], depending on the particular biological structure being imaged. Narrow dynamic line-width corresponds to long coherence length, which is necessary for applications which require a long imaging range such as whole eye imaging and meter scale industrial SS-OCT. Wide tuning range is also critical, because the axial spatial resolution in SS-OCT is inversely proportional to the laser tuning range[6]. With respect to gas spectroscopy, the laser properties outlined above provide a similar array of benefits. Narrow dynamic line-width is critical for resolving narrow spectral lines such as H_20/HF absorption features at low pressures. Wide tuning range provides access to a greater variety of lines and higher powers enable detection of lower concentrations.

* vijay@praevium.com. phone:805-448-4008

Smart Sensors, Actuators, and MEMS VI, edited by Ulrich Schmid, José Luis Sánchez de Rojas Aldavero, Monika Leester-Schaedel, Proc. of SPIE Vol. 8763, 87630H · © 2013 SPIE
CCC code: 0277-786X/13/$18 · doi: 10.1117/12.2018345

Downloaded From: http://proceedings.spiedigitallibrary.org/ on 04/16/2014 Terms of Use: http://spiedl.org/terms

Variable sweep rate/tuning range benefits gas spectroscopy by enabling a flexible instrument capable of charactering a variety of spectral ranges at varying levels of spectral resolution. Wavelength flexibility from near to mid-infrared wavelengths enables detection of a large variety of industrially important gases.

The features and benefits described above have spurred development of a diverse array of wavelength-swept source technologies in recent years, driven primarily by the increasing importance of SS-OCT in medical imaging, but also having relevance to gas spectroscopy. A comprehensive review of swept source options is found in Table I of a recent publication on ophthalmic imaging[5]. None of these prior approaches provides an ideal solution to the requirements outlined above, primarily because most prior devices have multiple longitudinal modes, which broadens dynamic line-width and shortens dynamic coherence length. Other limitations include fixed or limited sweep rate, wavelength inflexibility, or cost and complexity. Although integrated tunable lasers employed for telecommunications, such as the SGDBR laser[7], operate in a single longitudinal mode, tuning requires mode-hopping and multiple tuning electrodes, which is problematic for repetitive, high-speed wavelength sweeping applications. Additionally, although telecom tunable lasers provide sufficient tuning range for coverage of the communications C band (50nm around 1550nm), the range is still narrow by the standards of SS-OCT and some spectroscopic applications.

In 2009, Praevium Research, Advanced Optical Microsystems, commercial partner Thorlabs, and academic partner Massachusetts Institute of Technology (MIT) began developing a swept source based on amplified micro-electromechanical systems tunable vertical-cavity surface-emitting lasers (MEMS-VCSELs). The primary motivation for this effort was SS-OCT, but in recent years the applicability of these sources to transient spectroscopy has also been recognized and demonstrated. This partnership set out to create a truly single-mode, high power, high speed, widely tunable swept source for OCT, that was capable of variable sweep rates from the kHz range up to the MHz range with >100nm tuning. Target wavelength ranges included the 1310nm band for vascular, skin, and anatomic imaging, and the 1050nm band for ophthalmic imaging. MEMS-VCSELs promised an ideal swept source for following reasons. The short micron scale length of the VCSEL provides single-mode operation and rapid build-up time to lasing, and the low mirror mass in MEMS-VCSELs enables >1 MHz axial line rates. In addition, short-cavity designs have a longitudinal mode spacing well-exceeding 100nm, enabling mode-hop-free continuous tuning over >100nm. MEMS-VCSEL line-widths are tens of MHz[8], which corresponds to meter scale coherence lengths exceeding most current applications in medical SS-OCT, sufficient for industrial metrology, and sufficient for detection of critical gas absorption lines. Lastly, the fully integrated structure of the MEMS-VCSEL contrasts with the separation of gain and tuning elements present in prior external cavity lasers, suggesting both cost and performance benefits. Fixed wavelength VCSELs have already established themselves as a low-cost wafer-scale laser technology, and a MEMS-tunable device promises to exploit these same advantages.

MEMS-VCSELs were first conceived in the mid 1990s, but development efforts in the field until 2009 were driven primarily by telecommunications and narrow-tuning spectroscopic applications. Application of these devices to SS-OCT and transient spectroscopy therefore posed a large number of uncertainties. At that time, no MEMS-VCSELs had been demonstrated at the desired SS-OCT wavelength bands of 1310nm and 1050nm, though 1550nm devices had undergone advanced development for telecommunications applications. Secondly, the widest tuning range $\Delta\lambda$ reported for any MEMS-VCSEL at any wavelength was 65nm at λ=1550nm[9], corresponding to a fractional wavelength tuning $\Delta\lambda/\lambda$ of 4.2%. This is equivalent to 55nm at 1310nm, or less than half of what competing SS-OCT sources offered at that time. Thirdly, single-mode VCSEL output powers were limited to a few mW, short of the 30-60mW required for 1310nm applications and the 15-20mW required for 1050nm. Semiconductor-based optical amplification promised the required powers, but the quality of imaging obtainable with amplified VCSELs was unknown. Fourthly, although small signal and high speed tuning had been demonstrated in MEMS-VCSELs, high speed in conjunction with wide tuning range had never been simultaneously reported.

In the last 4 years, these challenges have been addressed and met through a large multi-disciplinary effort involving Praevium Research and its industrial and academic collaborators, as described in the following sections. A few highlights of this effort include the first MEMS-VCSELs at 1050nm and 1310nm, record tuning ranges of 150nm at 1310nm[10] and 100nm at 1050nm[11], whole eye imaging, anterior eye imaging, and retinal imaging with 1050nm VCSELs[5], Doppler blood flow imaging[12], the first application of SS-OCT to meter-scale imaging[13], and additional high quality images with both 1310nm and 1050nm VCSELs[14, 15]. Axial scan rates up to 1.2 MHz have additionally been demonstrated[14]. In addition, MEMS-VCSELs at 1310nm have been employed for high repetition rate molecular spectroscopy of HF and H_20[4], showing near transform-limited spectral performance and suggesting application to the most demanding low-pressure applications.

Downloaded From: http://proceedings.spiedigitallibrary.org/ on 04/16/2014 Terms of Use: http://spiedl.org/terms

2. 1310 AND 1050 NM VCSEL DEVICE STRUCTURE

Praevium Research and collaborators reported the first 1310nm MEMS-VCSELs in mid-2011[16], and the first 1050nm devices in early 2012[14]. Figure 1A illustrates a 3-dimensional solid model of a 1310nm MEMS-VCSEL[10]. The 1310nm epitaxial structure includes a wide-gain bandgap-engineered aluminum indium gallium arsenide (AlInGaAs) multi-quantum well (MQW) active region[17] epitaxially grown on an indium phosphide (InP) substrate, and joined by wafer bonding[18] to a wideband bottom gallium arsenide (GaAs)-based fully oxidized aluminum oxide ($GaAs/Al_xO_y$) bottom mirror[19]. Additional metal and dielectric layers on top of this "half-VCSEL" structure complete the optical cavity. This cavity includes a suspended top dielectric mirror, separated from the underlying half-VCSEL structure by an air gap, which can be contracted by electro-static force as a voltage is applied between the two actuator contacts shown. The VCSEL is optically pumped at 980nm through the top dielectric mirror, generating tunable 1310nm emission, which emerges from the top mirror and is fiber-coupled and amplified by a low-noise semiconductor optical amplifier (SOA) before being sent to an OCT system.

Figure 1B illustrates a similar view of a 1050nm device[11]. Here the gain region employs compressively strained indium gallium arsenide (InGaAs) quantum wells integrated with a $GaAs/Al_xO_y$ fully oxidized mirror. The structure requires no wafer-bonding, since the InGaAs quantum wells can be integrated by epitaxial growth with the GaAs-based mirror. In this case, the optical pump is at 850nm, generating tunable 1050nm emission.

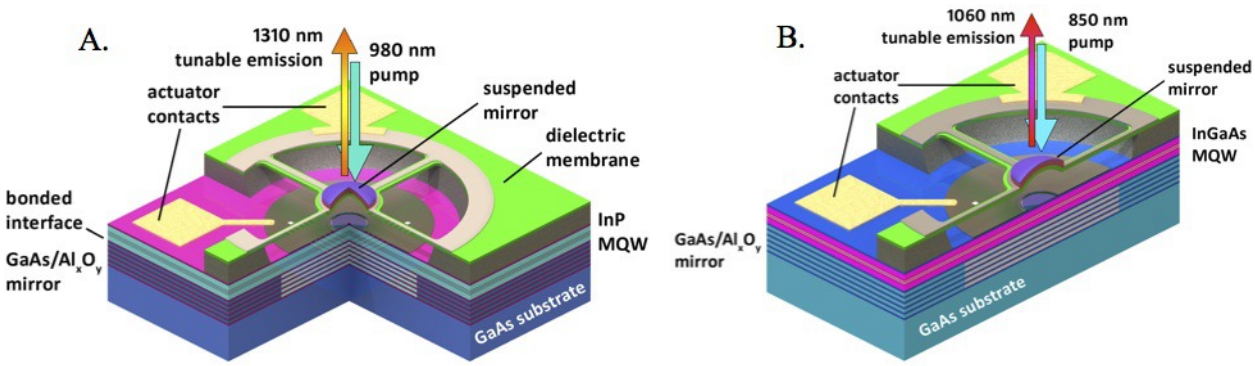

Figure 1: A. Solid model of 1310nm VCSEL structure. B. Solid model of 1050nm VCSEL structure.

Implicit in the device structures of Figs. 1A-B are a number of design choices that are critical to obtaining wide tuning range. One such choice is the use of optical instead of electrical pumping. Though the ultimate low-cost device will be electrically pumped, optical pumping can enhance tuning range for a number of reasons. First, the absence of electrically active dopants reduces absorption losses and thus leads to a corresponding reduction in threshold gain, enabling lasing over a wider portion of the available gain spectrum. Second, the absence of resistive heating associated with electrically pumped devices also increases available gain and again promotes wide tuning range. Third, optical pumping eliminates the need for thick intra-cavity current-spreading layers, allowing a thin optical cavity with wide free spectral range (FSR), promoting wide-range mode-hop free tuning.

Another critical design choice impacting tuning range and output power is the mirror structure. The top output mirror must have high mirror reflectivity (>99.6%) over a wide usable bandwidth (~150nm), and short optical field penetration, which reduces overall cavity thickness and widens FSR. The dielectric top mirror of the structure can employ commercially established materials such as SiO2/TiO2 or SiO2/Ta2O5, providing nearly 200nm of usable bandwidth. Equally important, however, is the bottom mirror, which for an efficient tunable VCSEL must have a higher mirror reflectivity of >99.9% over >200nm, and ideally with high thermal conductivity to enable efficient heat spreading and high output power. The fully oxidized mirror shown in Figs. 1A,B satisfies these requirements better than virtually any other mirror.

Downloaded From: http://proceedings.spiedigitallibrary.org/ on 04/16/2014 Terms of Use: http://spiedl.org/terms

3. MEMS ACTUATOR DESIGN CONSIDERATIONS

Design of the MEMS-based electro-static actuator shown in both the 1050 and 1310nm VCSELs of Figs 1A,B has significant impact on system performance of SS-OCT. For a flexible SS-OCT system, the MEMS actuator should have a flat and wide bandwidth frequency response, enabling operation at arbitrary scan rates and linearization of drive waveforms through control of higher frequency harmonics. (We focus here on electro-static rather than electro-thermal actuation, since the latter[20] does not provide speeds appropriate for SS-OCT or transient spectroscopy.) A scan that is linear with wavelength is highly desirable since this minimizes the bandwidth required of a subsequent analog to digital converter (A-D), which will sample the signal (either transmitted light in spectroscopy or interference fringe in SS-OCT) to generate an image (SS-OCT) or absorption spectrum (gas spectroscopy). Numerous parameters associated with the actuator geometry affect the MEMS-VCSEL tuning frequency response. These include the shape and lateral area of the actuator, the stress in the various layers comprising the suspended structure, and the thickness of the membrane and top DBR mirror. These parameters affect resonant frequency, damping, resulting bandwidth, voltage required for a given wavelength shift, and maximum achievable wavelength span. Many of these factors must be traded off to achieve a commercially viable design.

Our work has investigated a variety of geometries resulting in a variety of frequency responses, a sampling of which are illustrated in Fig. 2. The top left of the figure illustrates the range of frequency responses we have obtained by variation of the parameters discussed above. As shown, fundamental mode frequencies vary from about ~300kHz to ~500kHz, and damping varies from highly under-damped to near critically damped. Peak voltages for full tuning over one FSR (see representative results in Section 4 below), are around 60V. The flatter responses with 300kHz-500kHz resonance are preferable for linearizing the wavelength tuning response. The highest resonance devices have led to record axial line rates in SS-OCT of 1.2MHz, when both forward and backward wavelength scans are employed[14].

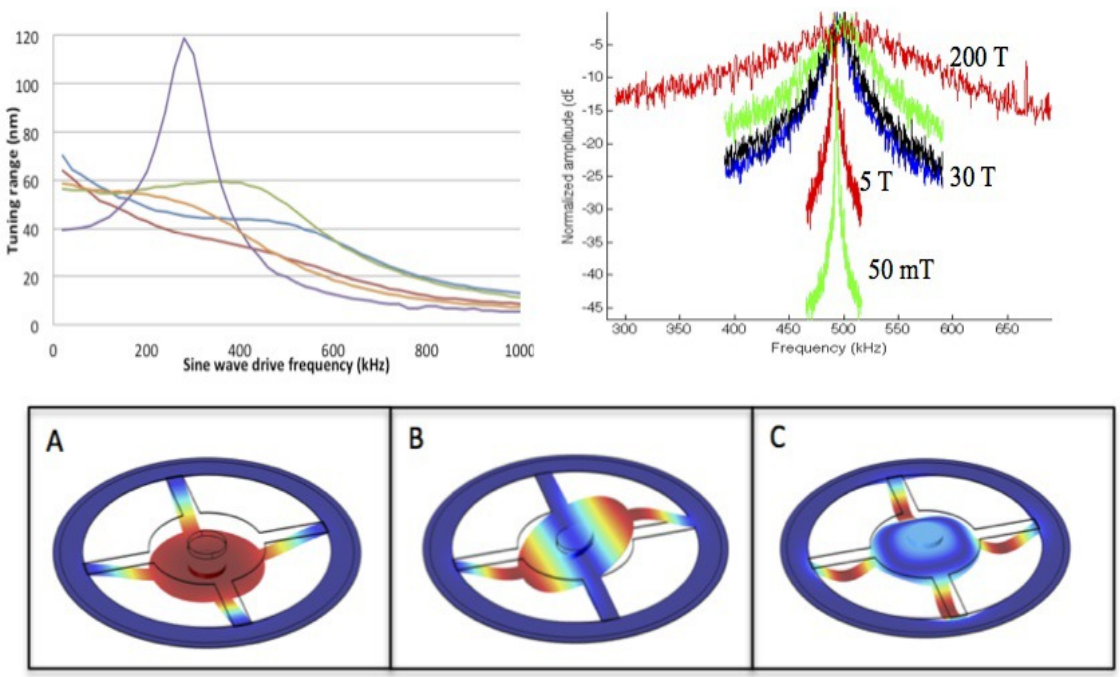

Figure 2: MEMS VCSEL frequency response. Top left shows various responses obtained from under-damped to near critically damped. Top right shows the impact of varying background pressure on MEMS-frequency response, for a single actuator design having ~480kHz resonance. Quality factor near 2000 is achieved at 50mT background pressure. Bottom row shows 3 lowest order modes of a 4-arm structure, including piston mode (A), tilt mode (B), and arm mode (C).

The responses illustrated in Figure 2 were all obtained at atmospheric pressure in air. The damping of the response is almost entirely dominated by interaction with viscous air, as illustrated in the top right of Fig. 2, which shows response as a function of background pressure for a device with a resonance near 480kHz. At low pressures such as 50mTorr, response is highly under-damped, showing a clear peak, and resonator quality factor increases from <10 at

Downloaded From: http://proceedings.spiedigitallibrary.org/ on 04/16/2014 Terms of Use: http://spiedl.org/terms

atmosphere to almost 2000 at 50 mT. Though this high Q value is not ideal for a flexible system requiring a variable scan rate, it does present a number of advantages for fixed scan rate applications, such as many commercial or clinical systems. First, the required voltage for full tuning range drops dramatically, from about 60V in an air structure to about ~3V in vacuum, which simplifies drive electronics. Linearization can be accomplished by overdriving and using only the linear portion of a sinusoidal sweep operated at resonance. Also, the absence of competing harmonics can lead to higher oscillator stability with lower phase noise.

The geometry of the MEMS actuator is sufficiently complex that accurate modeling requires a 3-D finite-element tool such as COMSOL™ to accurately predict frequency response and modal behavior. Finite element modeling also identifies some subtle features such as the impact of higher order modes on the dynamic response of the actuator. The bottom of Fig. 2 illustrates example COMSOL modeling of a typical suspended mirror employing a central plate and 4 supporting arms. The model reveals a lowest order "piston" mode shown in A, which is the primary peak seen in the responses at the middle left of the figure, and the motion desired for VCSEL tuning. Additionally shown is an undesirable tilting mode (B), and another undesirable mode corresponding to movement of the actuator arms with minimal movement of the central plate (C). These higher order modes can be excited by fabrication imperfections or higher drive harmonics used for linearization. Advanced MEMS characterization tools such as laser Doppler vibrometry[21] can help visualize actuator movement in real time, correlate with theoretical models, and adjust fabrication methods as necessary to achieve the desired movement.

4. MEMS-VCSEL PERFORMANCE

4.1 1310nm Devices

Figures 3 A-D illustrate some key static and dynamic tuning properties of ultra-broadband VCSELs at both 1310nm and 1050nm. The 1310nm devices of Fig. 3A,B[10] represent state of the art tuning ranges obtained in mid-2012, following up our first >100nm tuning ranges demonstrated in mid-2011[16]. In Figure 3A, the optical spectrum of a 1310nm VCSEL at an applied bias of ~12V is shown as the right-most red spectrum in the figure. This spectrum shows laser emission at 1372nm along with a competing mode at 1211nm, yielding a 161nm FSR for these devices. Application of a static voltage up to ~56V pulls the mode across a stable and continuous static tuning range of 142nm, illustrated by the overlaid spectra shown in Figure 3A. Higher applied biases enable further tuning to 1222nm (covering a 148nm range), though biases beyond ~56V exceed the static snap-down voltage of the device. Figure 3B shows the theoretical and measured static wavelength as a function of the applied tuning voltage. The green curve of Figure 3A shows the time-averaged optical spectrum under sinusoidal sweeping at 500kHz, illustrating a 150nm dynamic tuning range, which is more relevant than static tuning range for SS-OCT imaging. We note that this 500kHz sweep rate enables bi-directional scanning at rates >1MHz.

Devices similar to Fig. 3A-B with tuning range of 110-120nm are currently being commercialized for SS-OCT and have generated numerous SS-OCT images. These devices have also been employed in spectroscopy of HF and water vapor, as discussed in Section 6 below. We note that the 150nm tuning range shown above is the widest tuning range of any VCSEL at any wavelength reported to date. An electrically pumped 1550nm device employing electro-thermal actuation (limited to <1kHz and too slow for SS-OCT) demonstrated 102nm tuning range[20] around the same time as our first reported 110nm tuning range in optically pumped 1310nm devices.

4.2 1050nm Devices

The 1310nm devices reported first in mid-2011 were followed up by our report of the first 1050nm devices for ophthalmic imaging in early 2012[14]. A subsequent publication described device results in greater detail[11]. Figure 1B above illustrates the 1050nm device structure used for these devices. Figures 3C-D illustrate typical tuning behavior. In Fig. 3C, the zero voltage emission wavelength occurs at 1006nm. Application of a small bias causes the device to switch to the longer wavelength mode at ~1105nm. Further increases in the applied voltage reduce the emission wavelength to ~1010nm before the snap-down instability at approximately 53V inhibits further static tuning. Figure 3C illustrates an overlay of 11 spectra covering the >90nm static tuning range, demonstrating single longitudinal and transverse mode operation over the entire span. A wavelength range of 100nm, essentially equal to the free spectral range (FSR) of the cavity, can be accessed by dynamic tuning, as shown by the blue curve in Fig. 3C, which represents the time-averaged spectrum under repetitive sinusoidal sweeping at 200kHz. This dynamic tuning range is, again, the relevant wavelength span for repetitively swept SS-OCT applications. More recent devices have been operated at >500kHz sweep rates.

Downloaded From: http://proceedings.spiedigitallibrary.org/ on 04/16/2014 Terms of Use: http://spiedl.org/terms

The results in Fig. 3C-D represent the first 1050nm MEMS-VCSELs reported. Since then, electrically pumped devices with ~16nm tuning have been reported by another group[22].

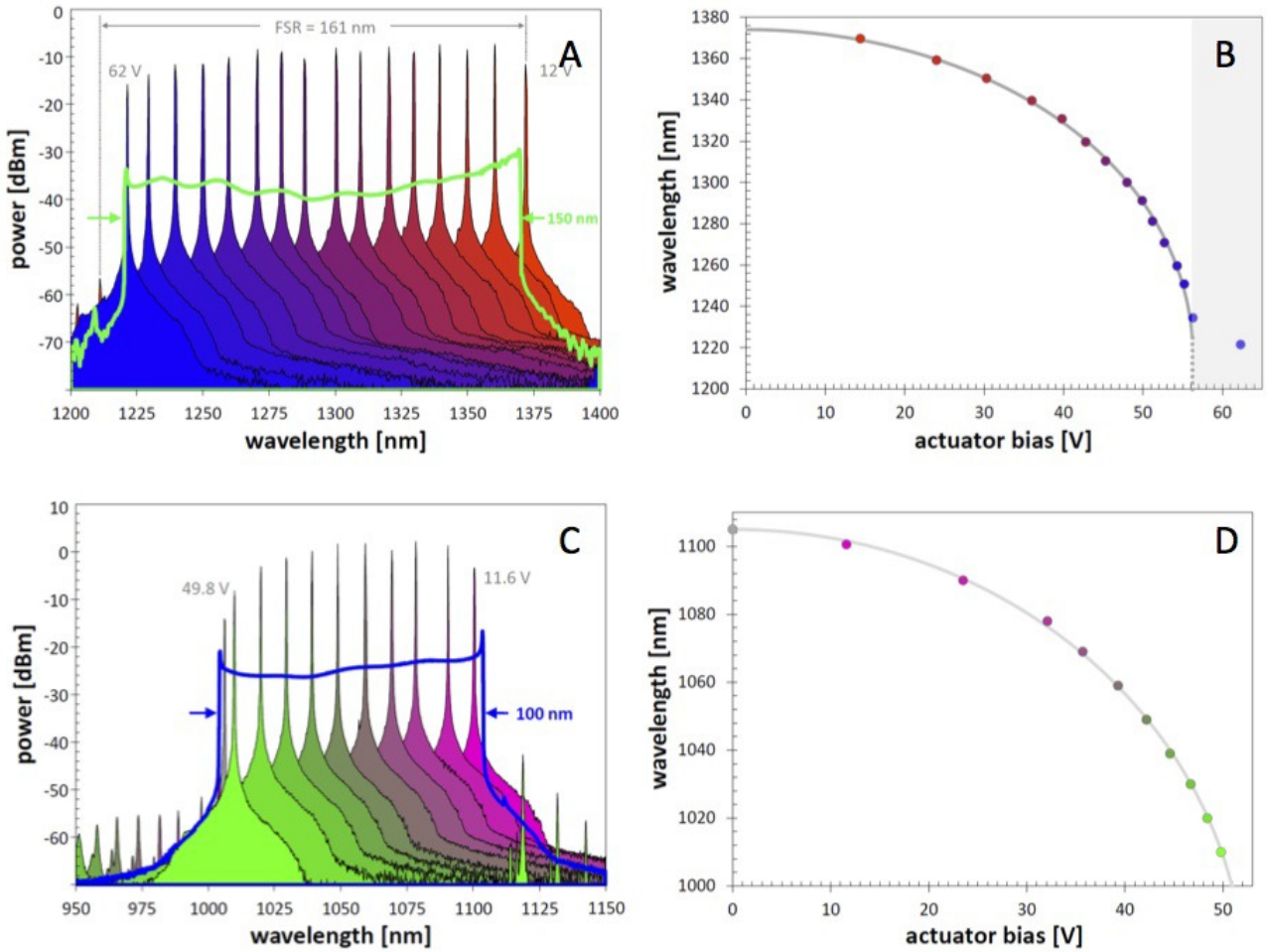

Figure 3: A. Static and dynamic spectra of 1310nm VCSEL with 150nm tuning range. Tuning range is 142nm under static operation, 150nm under dynamic operation, and cavity FSR is 161nm. B. Wavelength vs. applied voltage for 1310nm structure of Fig. 3A. C. Static and dynamic spectra of 1050nm VCSEL with 100nm tuning range. Tuning range is 90nm under static operation, 100nm under dynamic operation, and cavity FSR is 105nm. D. Wavelength vs. applied voltage for 1050nm device of Fig. 3C.

4.3 Additional performance parameters

Beyond static and dynamic tuning range, both 1050nm and 1310nm devices have demonstrated dynamic coherence lengths in excess of 1 meter and dynamic line-widths much less than several hundred MHz. These results are demonstrated primarily by system or fringe contrast measurements in SS-OCT, or by transform-limited gas line measurement in spectroscopy. Unlike a static line-width measurement, direct measurement of dynamic line-width or dynamic coherence length is complicated by the need for high speed electronics to measure either rapidly varying fringes in a long path intereferometer (SS-OCT coherence length measurement), or narrow spectral lines in a spectral transmission experiment (gas spectroscopy). All dynamic coherence length measurements to date have been electronics-limited, and the ultimate VCSEL coherence length may be much longer than the 1-2 meters thus far measured.

1050nm and 1310nm VCSELs also show constant polarization across the tuning range, also necessary for narrow dynamic line-width across the tuning range since different polarization modes may be at slightly different wavelengths. Other important performance achievements include linearized scanning and variable rate scanning, which have been demonstrated at both 1310nm and 1050nm[14]. Lastly, transverse mode suppression typically exceeds 45 dB in packaged

Downloaded From: http://proceedings.spiedigitallibrary.org/ on 04/16/2014 Terms of Use: http://spiedl.org/terms

devices. The primary parameter affecting the lateral mode suppression is the alignment of the pump beam to the fundamental mode. Careful attention to this during packaging can enable >45dB mode suppression over >100nm tuning at both 1050nm and 1310nm wavelengths.

5. APPLICATION TO SS-OCT IMAGING

The devices described in sections 2-4 above have been successfully employed in academic and commercial SS-OCT systems by collaborators at both MIT and Thorlabs, as described in detail in a number of recent publications[5, 12-15]. Figures 4A-I show a representative sample of images and illustrate the potential medical and industrial impact of this technology. Figures 4A-C were obtained with a 1050nm MEMS-VCSEL-based system operating at 580kHz axial scan rate[5]. Figure 4A illustrates the long dynamic coherence length of the VCSEL in a single image capturing both the anterior eye and the retina. Figure 4B shows a volumetric image of the choroid region from which the vascular cross-section in Fig. 4C can be constructed. Figure 4C is a color-coded image representing an overlay of both retinal and choroid vasculature systems, and is similar to images obtained using ICG angiography, but in a completely non-invasive MEMS-VCSEL-based OCT measurement requiring no injected dyes. Figures 4D-F illustrate the utility of MEMS-VCSEL for blood flow imaging which requires both very high scan speeds and phase stable operation[12]. Imaging blood flow may enable early detection of eye disease. Figure 4G illustrates a volumetric image of a rabbit stomach obtained using a 1310nm VCSEL operated at 1 MHz axial scan rate in conjunction with a miniaturized endoscopic probe[15]. This illustrates the potential utility of the MEMS-VCSEL in human endoscopic imaging. Figure 4H shows a photograph of a 6-inch tall optical post holder, and the Figure 4I is a volumetric OCT rendering of the same post holder, illustrating the ability to image inside a narrow deep bore hole[13]. These latter 2 figures illustrate the potential of SS-OCT to expand from its traditional use in short range medical imaging to longer-range industrial metrology, exploiting the long VCSEL coherence length.

6. APPLICATION TO HF AND WATER VAPOR SPECTROSCOPY

The application of MEMS-VCSELs to SS-OCT has thus far progressed faster than application to gas spectroscopy, primarily because this was the initial focus of the effort involving Praevium and its collaborators. Nevertheless, initial studies with collaborators at the University of Wisconsin at Madison demonstrate clear spectroscopic advantages of the high MEMS-VCSEL sweep speed coupled with superior dynamic line-width. Initial studies employed a 1310nm MEMS-VCSEL operated at 55kHz axial scan rate and over a tuning range of 33 nm from 1321-1354nm[4]. Although this sweep rate and tuning range do not make full use of the 1310nm VCSEL capability illustrated in Figure 3 above, no commercially available swept source currently exists in this wavelength range with the required performance[2]. This 1310nm VCSEL was used to measure ~790MHz wide low pressure HF and H_20 absorption lines, useful in engine thermometry of dynamic combustion engines.

Figure 5 illustrates absorbance spectra measured through an HF cell and H_20 cell connected in series. Figure 5A illustrates that measured HF and H_20 vapor lines match well with simulation. Figure 5B provides an expanded view near a single HF absorption line near 1340nm. At a sweep rate of 740 MHz/ns, corresponding to 55kHz sweep rate over 33nm, the measurement matches the simulation well, with the exception of a small asymmetry and subtle oscillations in the measured data. The source of this asymmetry is verified by sweeping the VCSEL wavelength at a much faster 12 GHz/ns, which accentuates the asymmetry and oscillations. These can be shown to be fundamental limitations associated with the Fourier transform limit of chirped pulses. Careful analysis of the measured spectral width indicates the VCSEL is providing near transform-limited spectral resolution[4].

Downloaded From: http://proceedings.spiedigitallibrary.org/ on 04/16/2014 Terms of Use: http://spiedl.org/terms

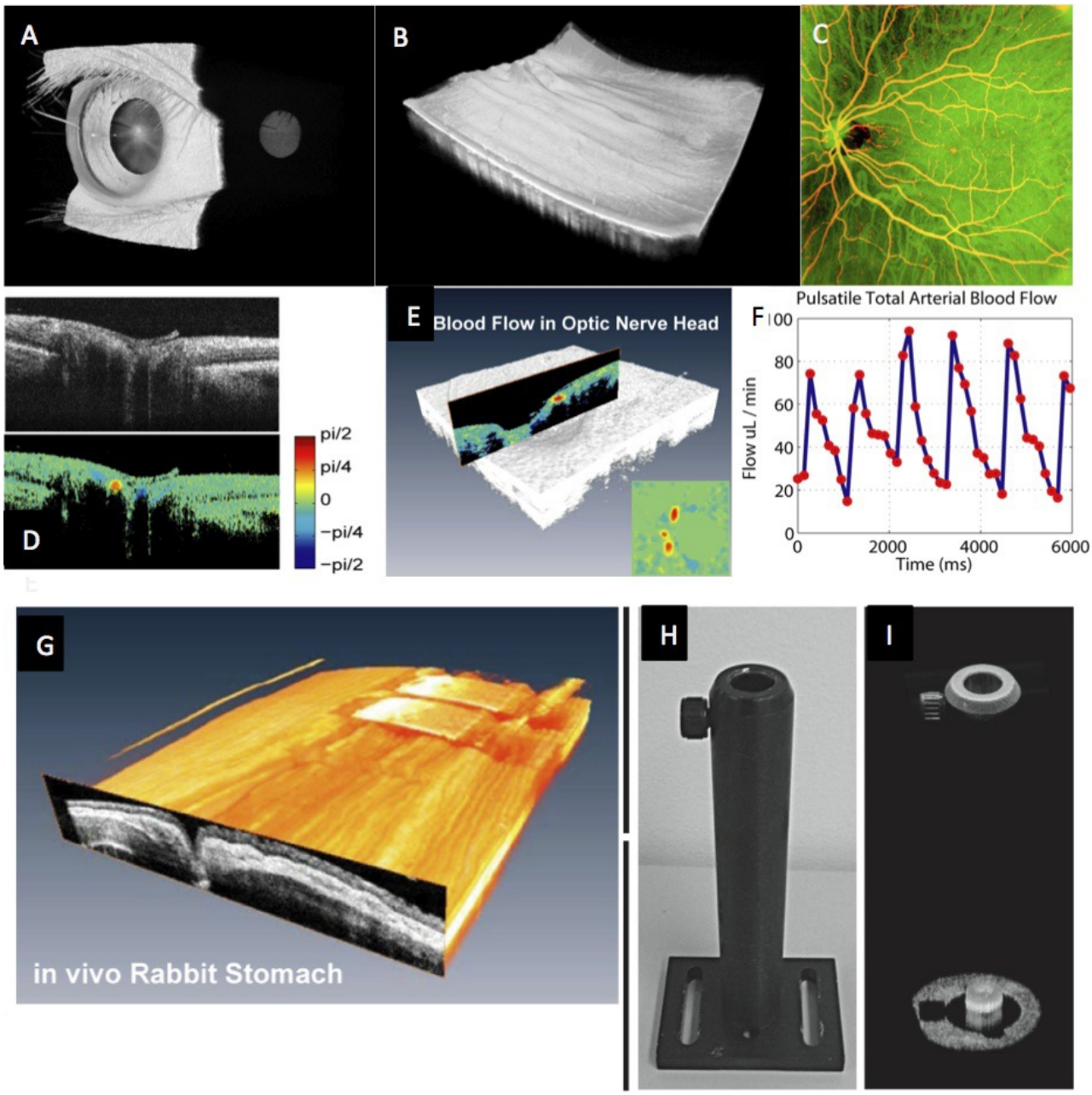

Figure 4: Representative OCT imaging results using 1050nm VCSEL (A-F, I) and 1310nm VCSEL (G). A. Full eye image showing anterior eye and retina in a single acquisition. B. Volumetric image of choroidal region. C. Choroidal and retinal vasculature superimposed and color-coded, from the data of B. D. OCT Intensity image and corresponding OCT doppler image of the optic nerve head in the retina obtained at 400 kHz axial scan rate. E. Representative 3-D volume of the optic nerve head from a rapidly acquired sequence of OCT volumes showing quantitative measurement of blood flow. F. Plot showing pulsatile blood flow into the eye obtained from analysis of multiple repeated 3D Doppler volumes of the optic nerve head. G. 1 MHz axial scan rate 3-D volume of in-vivo rabbit stomach obtained with a miniature endoscopic probe with a 1310nm VCSEL. H. Photograph of 6-inch tall optical post holder. I. OCT volumetric rendering of the optical post holder showing depth measurement of deep bore hole.

Downloaded From: http://proceedings.spiedigitallibrary.org/ on 04/16/2014 Terms of Use: http://spiedl.org/terms

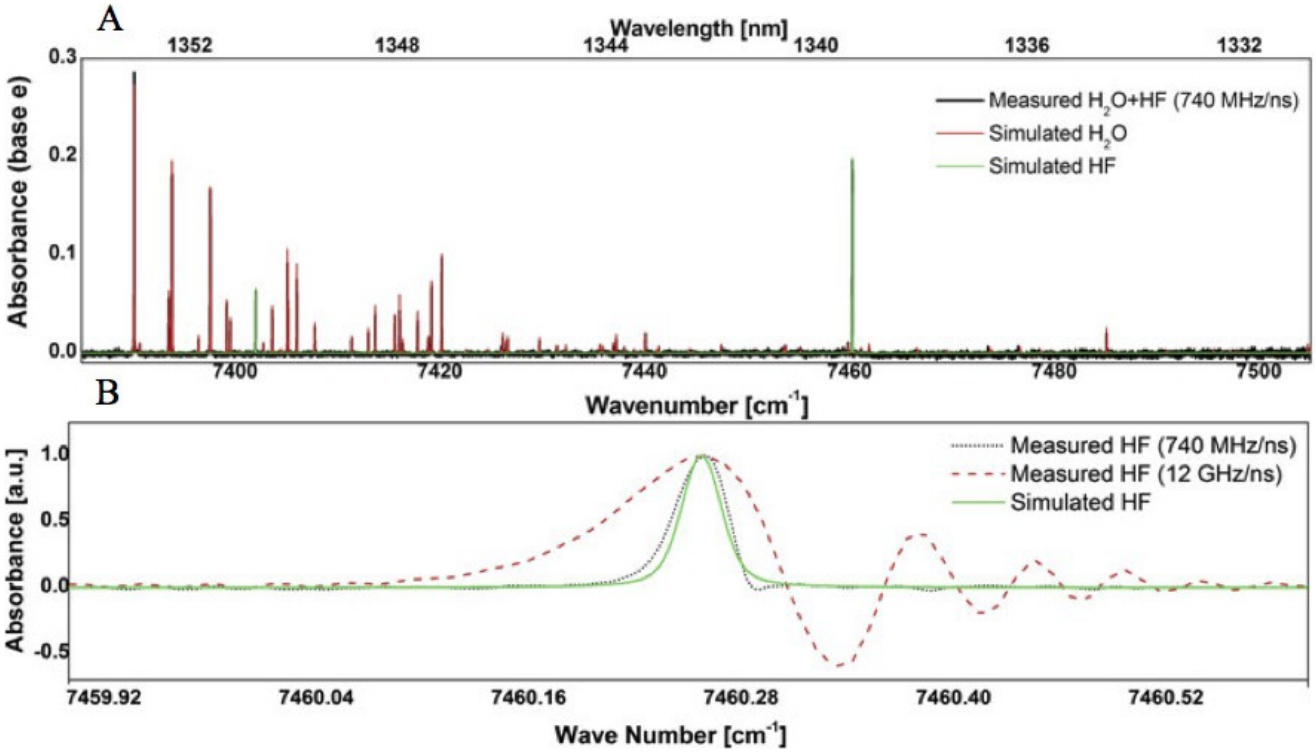

Figure 5: Measured HF and water vapor spectra from HF and H_20 cells in series[4]. A. Multiple absorption lines from 1330-1351 nm, using 1310nm VCSEL at 55kHz repetition rate, along with simulated expectations. B. Close up of ~1340nm line, illustrating effect of sweep speed and fundamental limits due to transform-limited chirped pulse width.

7. CONCLUSION

The last two years have seen dramatic improvements in MEMS-VCSEL tuning range and accessible wavelength bands, and the importance of these devices for imaging and spectroscopy has become increasingly evident. MEMS-VCSELs have enabled advancements in SS-OCT imaging speed and imaging range that were previously inconceivable with other swept sources. MEMS-VCSELs have also enabled identification of low-pressure gas absorption lines with near transform-limited accuracy.

A further advantage of the MEMS-VCSEL is wavelength flexibility, and migration of this technology to new wavelength regimes is an important future research direction. Fixed wavelength VCSELs have been demonstrated from as short as 450nm[23] to as long as 2300nm[24], with mid-infrared wavelengths up to about 4000nm potentially accessible. These suggest expansion of MEMS-VCSEL technology to the same wavelengths, enabling other kinds of spectroscopy.

Full realization of the low-cost potential of MEMS-VCSELs will require development of electrically pumped devices. Praevium Research is actively engaged in this effort, particularly at the 1050nm window, which could dramatically reduce the cost of ophthalmic imaging systems, and enable penetration of this technology into new clinical settings and economically disadvantaged nations.

ACKNOWLEDGMENTS

This work was supported by the National Institutes of Health (R01-EY011289-26, R01-EY013178-12, R01-EY013516-09, R01-EY019029-03, R01-CA075289-15, R01-NS057476-05, 1R44EY022864-01, R44-CA101067), Air Force Office for Scientific Research (FA9550-10-1-0551 and FA9550-10-1-0063), and Thorlabs. The content is solely the responsibility of the authors and does not necessarily represent the views of the Air Force or the NIH.

Downloaded From: http://proceedings.spiedigitallibrary.org/ on 04/16/2014 Terms of Use: http://spiedl.org/terms

REFERENCES

[1] Huber, R., Wojtkowski, M., Taira, K. *et al.*, "Amplified, frequency swept lasers for frequency domain reflectometry and OCT imaging: design and scaling principles," Optics Express, 13(9), 3513-3528 (2005).

[2] Sanders, S., "Wavelength-agile lasers," Optics & Photonics News, 16(5), 36-41 (2005).

[3] Adler, D. C., Chen, Y., Huber, R. *et al.*, "Three-dimensional endomicroscopy using optical coherence tomography," Nature Photonics, 1(12), 709-716 (2007).

[4] Stein, B. A., Jayaraman, V., Jiang, J. Y. *et al.*, "Doppler-limited H 2O and HF absorption spectroscopy by sweeping the 1,321-1,354 nm range at 55 kHz repetition rate using a single-mode MEMS-tunable VCSEL," Applied Physics B: Lasers and Optics, 108(4), 721-5 (2012).

[5] Grulkowski, I., Liu, J. J., Potsaid, B. *et al.*, "Retinal, anterior segment and full eye imaging using ultrahigh speed swept source OCTwith vertical-cavity surface emitting lasers," Biomed. Opt. Express, 3(11), 2733-2751 (2012).

[6] Choma, M. A., Sarunic, M. V., Yang, C. H. *et al.*, "Sensitivity advantage of swept source and Fourier domain optical coherence tomography," Optics Express, 11(18), 2183-2189 (2003).

[7] George, B., and Derickson, D., "High-Speed Concatenation of Frequency Ramps Using Sampled Grating Distributed Bragg Reflector Laser Diode Sources for OCT Resolution Enhancement," Proceedings of the SPIE - The International Society for Optical Engineering, 7554, (2010).

[8] Halbritter, H., Sydlo, C., Kogel, B. *et al.*, "Linewidth and chirp of MEMS-VCSELs," IEEE Photonics Technology Letters, 18(17-20), 2180-2182 (2006).

[9] Matsui, Y., Vakhshoori, D., Peidong, W. *et al.*, "Complete polarization mode control of long-wavelength tunable vertical-cavity surface-emitting lasers over 65-nm tuning, up to 14-mW output power," IEEE Journal of Quantum Electronics, 39(9), 1037-10481048 (2003).

[10] Jayaraman, V., Cole, G. D., Robertson, M. *et al.*, "High-sweep-rate 1310 nm MEMS-VCSEL with 150 nm continuous tuning range," Electronics Letters, 48(14), 867-9 (2012).

[11] Jayaraman, V., Cole, G. D., Robertson, M. *et al.*, "Rapidly swept, ultra-widely-tunable 1060 nm MEMS-VCSELs," Electronics Letters, 48(21), 1331-1333 (2012).

[12] WooJhon, C., Potsaid, B., Jayaraman, V. *et al.*, "Phase-sensitive swept-source optical coherence tomography imaging of the human retina with a vertical cavity surface-emitting laser light source," Optics Letters, 38(3), 338-40 (2013).

[13] Grulkowski, I., Liu, J. J., Potsaid, B. *et al.*, "High-precision, high-accuracy ultralong-range swept-source optical coherence tomography using vertical cavity surface emitting laser light source," Optics Letters, 38(5), 673-675 (2013).

[14] Potsaid, B., Jayaraman, V., Fujimoto, J. G. *et al.*, "MEMS tunable VCSEL light source for ultrahigh speed 60kHz - 1MHz axial scan rate and long range centimeter class OCT imaging," Proceedings of the SPIE - The International Society for Optical Engineering, 8213, (2012).

[15] Tsai, T. H., Tao, Y. K., Potsaid, B. *et al.*, "Ultrahigh speed endoscopic optical coherence tomography using micro-motor imaging catheter and VCSEL technology," Proceedings of the SPIE - The International Society for Optical Engineering, 8571(85710N), (2013).

[16] Jayaraman, V., Jiang, J., Li, H. *et al.*, "OCT Imaging up to 760 kHz Axial Scan Rate Using Single-Mode 1310nm MEMS-Tunable VCSELs with >100nm Tuning Range," CLEO: 2011 - Laser Science to Photonic Applications, 2 pp.-2 pp.2 pp. (2011).

[17] Zah, C. E., Bhat, R., Pathak, B. N. *et al.*, "High-performance uncooled 1.3-um Al(x)Ga(y)In(1-x-y)As/InP strained-layer quantum-well lasers for subscriber loop applications," IEEE Journal of Quantum Electronics, 30(2), 511-523 (1994).

[18] Black, A., Hawkins, A. R., Margalit, N. M. *et al.*, "Wafer fusion: Materials issues and device results," IEEE Journal of Selected Topics in Quantum Electronics, 3(3), 943-951 (1997).

[19] MacDougal, M. H., Dapkus, P. D., Bond, A. E. *et al.*, "Design and fabrication of VCSELs with Al xO y-GaAs DBRs," IEEE Journal of Selected Topics in Quantum Electronics, 3(3), 905-915915 (1997).

[20] Gierl, C., Gruendl, T., Debernardi, P. *et al.*, "Surface micromachined tunable 1.55 mu m-VCSEL with 102 nm continuous single-mode tuning," Optics Express, 19(18), 17336-17343 (2011).

[21] Turner, K. L., Hartwell, P.G., MacDonald, N.C. , "Multi-dimensional MEMS motion characterization using laser vibrometry," Digest of Technical Proceedings: Transducers, '99: The 10th international conference on solid state Sensors and Actuators, 1144-1147 (1999).

Downloaded From: http://proceedings.spiedigitallibrary.org/ on 04/16/2014 Terms of Use: http://spiedl.org/terms

[22] Ansbaek, T., Chung, I.-S., Semenova, E. S. *et al.*, "1060-nm Tunable Monolithic High Index Contrast Subwavelength Grating VCSEL," IEEE Photonics Technology Letters, 25(4), 365-367 (2013).
[23] Higuchi, Y., Omae, K., Matsumura, H. *et al.*, "Room-Temperature CW Lasing of a GaN-Based Vertical-Cavity Surface-Emitting Laser by Current Injection," Applied Physics Express, 1(12), (2008).
[24] Boehm, G., Bachmann, A., Rosskopf, J. *et al.*, "Comparison of InP- and GaSb-based VCSELs emitting at 2.3 mu m suitable for carbon monoxide detection," Journal of Crystal Growth, 323(1), 442-445 (2011).

Downloaded From: http://proceedings.spiedigitallibrary.org/ on 04/16/2014 Terms of Use: http://spiedl.org/terms